Journal of Polymer Research (2020) 27: 366
https://doi.org/10.1007/s10965-020-02331-x

Polypyrrole nanoparticles: control of the size and morphology

Monika Paúrová[1] · Ivana Šeděnková[1] · Jiřina Hromádková[1] · Michal Babič[1]

Received: 7 January 2020 / Accepted: 21 October 2020 / Published online: 12 November 2020

Abstract
A method of controlling the size and morphology of polypyrrole nanoparticles (PPy-NPs) is successfully developed by using the combination of various non-ionic and anionic surfactants and polymerization temperatures during the synthesis. Uniform PPy-NPs are prepared via water-based redox heterogeneous polymerization of pyrrole in the presence of ammonium persulphate as an oxidant. The properties of the prepared materials are evaluated by a transmission electron microscopy and dynamic light scattering in terms of particles morphology, colloidal stability, zeta potential and hydrodynamic size and distribution. Raman, infrared and UV–Vis spectral characteristics of the particles are used to elucidate structural and optical properties of PPy-NPs. The size and morphology of polypyrrole nanoparticles prepared by a polymerization of pyrrole with ammonium persulphate can be controlled by various types and concentrations of surfactants with the hydrophilic-lipophilic balance values between 10−16 and also by the polymerization temperature. Spectroscopic studies confirm that the surfactants can be washed out from the surface, although some residues remain enclosed inside particles matrix.

Keywords Polypyrrole · Nanoparticles · Heterogeneous polymerization · Polymer colloids

Introduction

In recent decades, conducting polymers [1, 2], mainly polypyrrole, have received considerable attention for their use as attractive multifunctional materials in many scientific and technological fields. These applications include chemical and biological sensors [3, 4], polymeric rechargeable batteries [5], electro-chromic windows and displays [6], corrosion protection materials [7], functional separation membranes [8], absorbents for heavy metal ions [9], etc. Additionally, polypyrrole nanoparticles (PPy-NPs) have also become one of the most studied materials for biomedical applications due to their desirable chemical and physical properties, such as their biocompatibility towards proteins, DNA and the immune system of mammals [10–12], environmental stability in atmospheric conditions, good chemical and high photo-stability and simplicity of preparation. In addition to their use as scaffolds for tissue engineering [13], drug delivery systems and contrast or photothermal agents [14–17] for both diagnostic and therapeutic applications, polypyrrole could be applied for the modification of inorganic nanoparticles [18, 19] and used as a suitable layer for other biological modifications.

Conducting polymers could be prepared by a number of methods, including electrochemical polymerization [20–22], chemical polymerization [23–25] and UV-induced radical polymerization [26, 27]. Using a chemical approach to prepare colloidal polymeric nanoparticles is the most efficient and attractive way to achieve the required properties of the prepared material. The rate and agitation of polymerization, reaction time and temperature, pH in solution, amount and molecular weight of a surfactant/stabilizer, character of the doping anion, type of oxidant, ratio of the oxidant to the monomer concentration, and solvent type are the factors that can easily change and influence the morphology and size of the prepared polymeric nanoparticles [28]. Many types of oxidants, iron(III) salts [29–32], persulphate anions [33–35], hydrogen peroxide [36, 37], potassium permanganate [38], potassium dichromate [39], potassium ferricyanide(III) [40], potassium iodate [41], silver nitrate [42], gold nanoparticles

Electronic supplementary material The online version of this article (https://doi.org/10.1007/s10965-020-02331-x) contains supplementary material, which is available to authorized users.

✉ Michal Babič
babic@imc.cas.cz

[1] Institute of Macromolecular Chemistry, Czech Academy of Sciences, Heyrovského nám 2 162 06, Prague 6, Czech Republic

[19] and many other reagents have been used in reactions described in the literature.

To prevent the macroscopic aggregation of the resulting material during polymerization or subsequent storage, stable colloidal PPy-NPs or composites were prepared in the presence of stabilizers, typically water-soluble polymers or surfactants [43]. Sodium dodecyl sulphate [34, 35, 44], polyvinylpyrrolidone [26, 45, 46], poly(vinyl alcohol) [47–49], poly(ethylene glycol) [50, 51] or sodium dodecylbenzenesulphonate [52] were most frequently investigated by many scientific groups. Apart from aggregation, the effect of the stabilizer charge on the conductivity, morphology or resulting chemical properties was also fully studied. For example, Omastová et al. [32] provided a deeper insight on the performance of anionic, cationic and non-ionic surfactants during the chemical oxidative synthesis of PPy in aqueous media with ferric salt. They concluded that anionic surfactants were incorporated into the PPy structures as doping anions. In addition, Hoshina et al. [53] described the influence of the agitation speed and different types of charged surfactants on the conductivity and particle size of powder materials obtained by emulsion polymerization. In other work, Kwon et al. [54] examined the chemical and physical properties of a PPy material prepared in the presence of a mixed surfactant system. They used a combination of the anionic surfactant dodecylbenzene sulphonic acid and non-ionic surfactant Triton X-100 (polyethylene glycol *p*-(1,1,3,3-tetramethylbutyl)-phenyl ether).

However, further works concerning the effect of polysorbate-based non-ionic emulsifiers (TWEENs) on the colloidal stability of formed PPy nanoparticles rather than of bulk PPy powders have not been extensively described in the literature. In addition, a description of the temperature influence on the particles size and morphology in the presence of a non-ionic surfactant is missing as well. Recently, polypyrrole particles seem to be promising candidates for use as contrast agents for photoacoustic tomography (imaging) [14–17]. The use of polymer contrast agents could overcome some difficulties of using low-molecular contrast agents, such as photobleaching and the weakening of the signal due to the diffusion of the contrast agent into the interstitium or across tissues. Thus, the control of the size and dispersity of particles is crucial for determining their behavior *in vivo*, e.g., the biological half-life, clearance, specific tissue targeting, etc. Therefore, the presented work is focused on the development of methods of controlling the size and surface properties of PPy-NPs by a one-step oxidative polymerization mediated by ammonium persulphate. Effects of the different types and concentration of various surfactants or polymer stabilizers (hydrophilic-lipophilic balance – HLB* values of used surfactants are in range 10.5–40) and polymerization temperature on the size, morphology and colloidal stability of nanoparticles are investigated. The behavior of the colloidal dispersions was examined by dynamic light scattering (DLS), and the morphology of the colloids was studied by transmission electron microscopy (TEM). Infrared/Raman spectroscopy and UV–Vis spectroscopy were used to characterize the particles as well.

* *HLB is a semiempirical quantitative description of surfactant ability to stabilize a certain type of an emulsion. It is defined as a balance of the size and strength of the hydrophilic and lipophilic (hydrophobic) moieties of a surfactant molecule. For example, surfactants with low HLB values acts as w/o emulsifiers and those with higher HLB acts as o/w emulsifiers* [55–60]. *For more details see Supporting information (S).*

Experimental section

Materials

All the chemicals, except pyrrole, were used as received. Pyrrole (Py, reagent grade 98%, was dried by CaH_2 and purified by distillation in vacuo and stored in a refrigerator at approximately 4 °C before use), sodium dodecyl sulphate (SDS), sodium docusate (AOT), polyoxyethylene (PEG, $M_n = 4000$), poly(ethylene glycol) sorbitan monolaurate (TWEEN 20), polyoxyethylenesorbitan monopalmitate (TWEEN 40), poly(ethylene glycol) sorbitan monostearate (TWEEN 60), poly(ethylene glycol) sorbitan monooleate (TWEEN 80), polyvinylpyrrolidone (PVP, $M_n = 40\ 000$), ammonium persulphate ($(NH_4)_2S_2O_8$, APS, reagent grade ≥ 98%), iron(III) chloride hexahydrate ($FeCl_3 \cdot 6H_2O$, reagent grade ≥ 98%), and PBS buffer (phosphate buffered saline tablet) were purchased from Sigma-Aldrich. Glycerol was purchased from Penta (Praha, Czech Republic), and hydrogen peroxide (H_2O_2, 30%, un-stabilized) was purchased from Lachner (Neratovice, Czech Republic). Deionized water (18.2 MΩ cm) obtained from a water purification system (Purelab Ultra) was used in all the preparation processes.

Synthesis of the PPy-NPs

PPy-NPs were synthesized by the differently stabilized chemical oxidative polymerization of pyrrole monomers with ammonium persulphate used as an oxidant.

In a typical procedure, the reactions were performed in 30 ml septum-sealed flasks on a magnetically stirred thermoblock at various temperatures. First, a specific amount of an anionic surfactant (SDS or AOT) or a non-ionic stabilizer (glycerol, PVP, PEG, TWEEN 20, TWEEN 40, TWEEN 60 or TWEEN 80, 5–200 mm, 0.1–10 wt%) was dissolved in 17 ml of deionized water. Consequently, the pyrrole monomer (Py, 51.7 μL, 0.74 mmol, was added to the solution

and stirred for 20 min. After that, $(NH_4)_2S_2O_8$ solution was added dropwise (168 mg in 3 ml in water, 0.74 mmol, molar ratio of Py to the oxidant was set to 1/1) to the reaction mixture under stirring. After a while, the colorless system gradually became black; the polymerization was allowed to proceed for 24 h at room temperature (stirring at 500 rpm) or at 3 °C, 40 °C, 55 °C, 70° or 85 °C. The temperature-dependent experiments were performed only with 1 wt% non-ionic PVP stabilizer and TWEEN 40, 60 and 80.

For the UV–Vis analysis, the polymerizations were performed in 1 wt% PVP. $FeCl_3$, H_2O_2 and APS were used as the oxidants in two molar ratios (the molar ratio of Py to the oxidant was set to $n_{Py}/n_{oxidant} = 1/1$ and 1/2.3) to oxidize Py (51.7 µL, 0.74 mmol).

After polymerization, the PPy-NPs were washed by centrifugation with deionized water (8 times, for 1.5 h, 25 °C, 7830 rpm) and sonicated for 1 min.

Characterization of the PPy-NPs

The size and morphology were directly evaluated from the microphotographs (using at least 300 particles) obtained by a transmission electron microscope (FEI-TEM, Tecnai G2 Spirit, Oregon, USA). The TEM data were analyzed with ImageJ analysis software. The samples washed for the TEM analysis were prepared by depositing a diluted aqueous PPy-NPs dispersion on a grid with a copper membrane and carbon film and dried at room temperature.

The hydrodynamic diameter (D_h), polydispersity index (PI) and zeta potential (ζ) were measured by dynamic light scattering (DLS, Zetasizer Nano Series ZEN3500, Malvern, Worcestershire, UK). For all the analyses, the diluted aqueous PPy-NPs dispersions were measured in disposable folded DTS1070 capillary cells.

The UV–Vis spectra of the aqueous dispersion of the washed particles (in physiological PBS buffer, pH = 7.4) were measured on a UV spectrophotometer (Analytic Jena Specord® 210 Plus, Jena) using quartz cuvettes with an optical path of 1 cm and a wavelength range of 190–1100 nm.

The Fourier transform infrared (FTIR) spectra of the PPy-NPs powder (prepared without a surfactant/stabilizer and lyophilized from the aqueous dispersion) in potassium bromide pellets were obtained from 64 scans with a resolution of 2 cm^{-1} using a Thermo Nicolet NEXUS 870 FTIR spectrometer (Madison, WI, USA). The liquid samples of the emulsifiers/stabilizer were measured using an ATR Golden Gate diamond prism unit (Specac Ltd., Orpington, UK). The spectra were obtained in a dry-air-purged environment and corrected for the presence of carbon dioxide and residual water vapor in the optical path.

The Raman spectra excited with a diode near infrared laser with $l = 785$ nm were collected on a Renishaw inVia Reflex Raman microscope (Renishaw Plc., New Mills, UK). A research grade Leica DM LM microscope equipped with a 50 × Olympus objective lens was used to focus the laser beam on the sample. The scattered light was analyzed using a spectrograph with a holographic grating density of 1200 lines nm^{-1}. A Peltier cooled CCD detector registered the dispersed light.

Results and discussion

Synthesis of the PPy-NPs

A set of experiments was carried out to examine the effect of various types/concentrations of anionic surfactants and non-ionic polymer stabilizers on the particle size and surface morphology (Table 1).

PEG and PVP polymers were used in the reactions as stabilizers to protect the particles against aggregation via increasing the colloid viscosity and steric stabilization by adsorbing of stabilizers on the particle surfaces. To fully understand the synergy of these two effects, glycerol with no steric stabilization effect was used here only to change the viscosity. The experiments with glycerol, PEG and TWEEN 20 were found to be unsuccessful since the reactions produced an undesirable coagulum precipitate of bulky PPy particles. In contrast, the use of PVP and a polysorbate-based stabilizer/emulsifier, not including TWEEN 20, allowed good particle size and polydispersity control (Table1). In the case of non-ionic surfactants and polymer stabilizers, only substances with HLB values within the range 10–16 can be used for the sufficient stabilization of the growing PPy-NPs. The use of non-ionic stabilizers with HLB values higher than 16 led to coagulation of PPy-NPs. On the other hand, the anionic surfactants (SDS and AOT) were found to be good stabilizers of PPy-NPs dispersion despite their high HLB values. This behavior can be ascribed to their

Table 1 Observation results of the reaction mixture after polymerization[a)]

Surfactant	Concentration	Observation	HLB [60]
SDS	5–200 mM	stable colloid dispersion	36.4
AOT	5–200 mM	stable colloid dispersion	32.0
glycerol	0.1–10 wt%	precipitating coagulum	20.0
PEG	0.1–10 wt%	precipitating coagulum	18.5
TWEEN 20	0.2–8 wt%	precipitating coagulum	17.0
TWEEN 40	0.2–8 wt%	stable colloidal dispersion	15.6
TWEEN 60	0.2–8 wt%	stable colloidal dispersion	15.0
TWEEN 80	0.2–8 wt%	stable colloidal dispersion	15.0
PVP	0.1–10 wt%	stable colloidal dispersion	10.5

[a)] molar ratio $n_{Py}/n_{oxidant} = 1/1$, $(NH_4)_2S_2O_8$ was used as an oxidant, room temperature, 24 h.

anionic character, due to which these substances act not only as very potent o/w emulsifiers, but also as solubilizers. Their sulphate groups generate dielectric repulsive forces, which results in good stabilization of discrete phases in aqueous systems.

In addition to commonly used $FeCl_3$, APS and H_2O_2 were tested as oxidants. The reason of that was a known fact, that rising valence of ions affects negatively a stability of water-based dispersions (Fe^{3+} cation is an effective emulsion breaker). Especially the use of APS allowed an employment of classical emulsifiers besides polymer stabilizers, what resulted in better colloidal stability and control of PPy-NP size.

Characterization of the PPy-NPs

DLS analysis

The hydrodynamic diameter D_h, polydispersity index PI and zeta potential was determined by DLS. The experiments confirmed that the size of the nanoparticles decreased when the surfactant concentration increased, while the concentration of the monomers and oxidant was constant (Fig. 1 and Fig. 2). The use of anionic and non-ionic surfactants during polymerization at concentrations above a critical micellar concentration (CMC) allowed good control of the particles size and polydispersity, as well as PVP polymer stabilizer (Fig. 1 and Table S1). Below the CMC, the PPy-NPs tended to form coagulum. Values of zeta potential (ζ) of the PPy-NPs in diluted aqueous dispersions (pH = 3, 25 °C) was found to be between + 4 and + 12 mV for the PPy-NPs prepared with the polysorbate-based emulsifiers and almost a neutral charge was observed for the particles prepared in PVP (Fig. 1 and Table S1). The colloidal stability at low ζ values could be explained with the formation of very small particles, which are affected by hydrodynamic forces more than by gravitation. Moreover, non-ionic surfactants with HLB values within the range 10–16 can effectively hinder PPy-NPs from coalescence and coagulation during the preparation and storage, what plays important role in dispersion stability in general.

DLS measurement also showed that, oxidant type did not play a significant role in sense of stable dispersion formation, when PVP was used as steric polymer stabilizer. Similar ζ

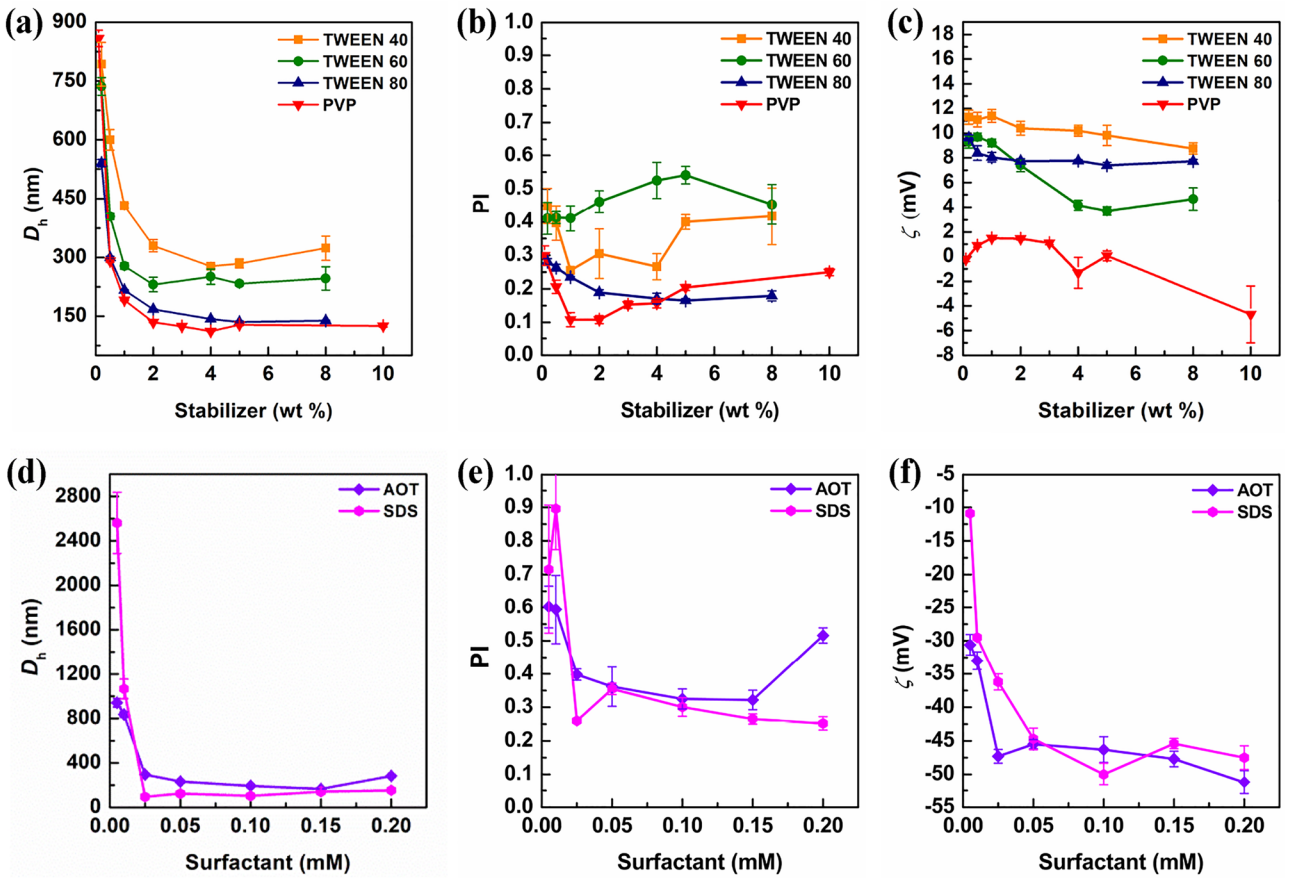

Fig. 1 (**a**) and (**d**) Hydrodynamic diameters, (**b**) and (**e**) polydispersity index, and (**c**) and (**f**) zeta potential of the PPy-NPs dispersed at a pH ~ 3.0 and 25 °C using APS as an oxidant (1/1) as a function of the concentration of the stabilizer/surfactant, as determined by DLS

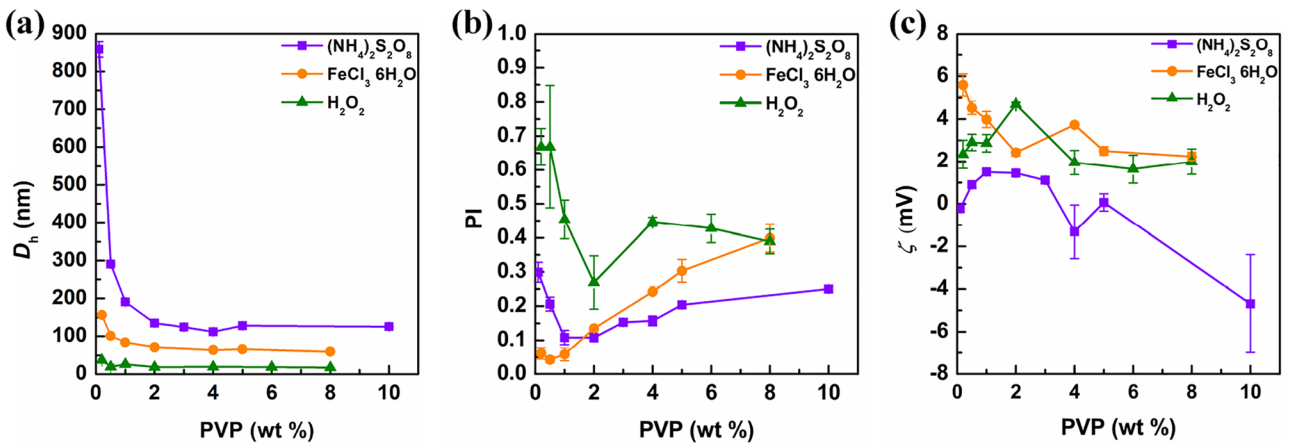

Fig. 2 **(a)** Hydrodynamic diameter, **(b)** polydispersity index, and **(c)** zeta potential of the PPy-NPs dispersed at a pH ~ 3.0 and 25 °C using APS, $FeCl_3$ or H_2O_2 as an oxidant (1/1) as a function of the PVP concentration, as determined by DLS

values were found as well, when $FeCl_3$ and H_2O_2 oxidizers were used instead of APS together with PVP (Fig. 2 and Table S2). It indicates a formation almost non-polarized (uncharged) polymer particles cores, what was consequently confirmed by FTIR measurements (see chapter 3.2.4.).

TEM analysis

The morphology of the resulting polymer nanoparticles was studied by transmission electron microscopy. The number-average particle diameter and weight-average particle diameter (D_n and D_w, respectively) and dispersity $Đ$ [61] were calculated from the TEM microphotographs using the following equations:

$$D_n = \frac{n_i D_i}{n_i} \tag{1}$$

$$D_w = \frac{\sum_i n_i D_i w_i}{\sum_i n_i w_i} = \frac{\sum_i n_i D_i \rho V_i}{\sum_i n_i \rho V_i} = \frac{\sum_i n_i D_i \rho \frac{1}{6}\pi D_i^3}{\sum_i n_i \rho \frac{1}{6}\pi D_i^3} = \frac{\sum_i n_i D_i^4}{\sum_i n_i D_i^3} \tag{2}$$

$$Đ = \frac{D_w}{D_n}; < 1, \infty) \tag{3}$$

where n_i is the number of particles, D_i is the diameter of the nanoparticles, w is the weight, ρ is the density and V is the volume. At least 300 nanoparticles were examined for each sample.

The typical transmission electron micrographs represent general morphological features of the PPy-NPs, which were obtained using PVP stabilizer or various non-ionic/anionic surfactants during polymerization (Fig. 3).

The transmission electron microscopy (TEM) results showed that the morphology of the nanoparticles changed from spherical to slightly elliptical shapes with increasing the HLB value. Water-soluble PVP and polysorbate-based stabilizer/emulsifiers with HLB values within the range 10–16 demonstrated nearly monodisperse systems with average sizes ranging from 35 to 75 nm and regular spherical nanoparticles (Fig. 4b, Fig. S1). When the non-ionic Tween 20 and PEG were used (HLB values > 16), the immediate and significant aggregation of the bulky PPy particle during polymerization was observed (Table 1, TEM morphology was immeasurable). On the other hand, anionic surfactants SDS and AOT with the highest HLB values allowed a preparation of very stable colloids resistant to aggregation. However, TEM micrographs showed irregular aggregates (Fig. 3e and Fig.3f) consisting of particles with imperceptible interfaces between the individual particles. It can be suggested that well dispersed particles underwent a coalesce during a drying on the TEM copper grid. This can be explained in terms of high HLB values of SDS and AOT. Although they stabilized the growing PPy-NPs very effectively, a significant reduction of the surface tension on the particle interfaces (partial solubilization effect) resulted in a lower polymer density in the particles. It made particles softer and prone to coalescence (sintering) during an evaporation of dispersing media. Therefore, in this case, particle size analyses from TEM micrographs were not made. This explanation is also in accordance with an observation of Omastová [32], who confirmed the presence of SDS as an associating sulphate counter-ion inside the bulk PPy. It was thus summarized, that surfactants with HLB values lower than 16 should be used for the formation of hardy and resistant particle surfaces.

Additionally, all the TEM analyses confirmed that the size of the PPy-NPs decreased and their water-dispersion stabilities increased with increasing concentration of the used surfactant/stabilizer. This is also in agreement

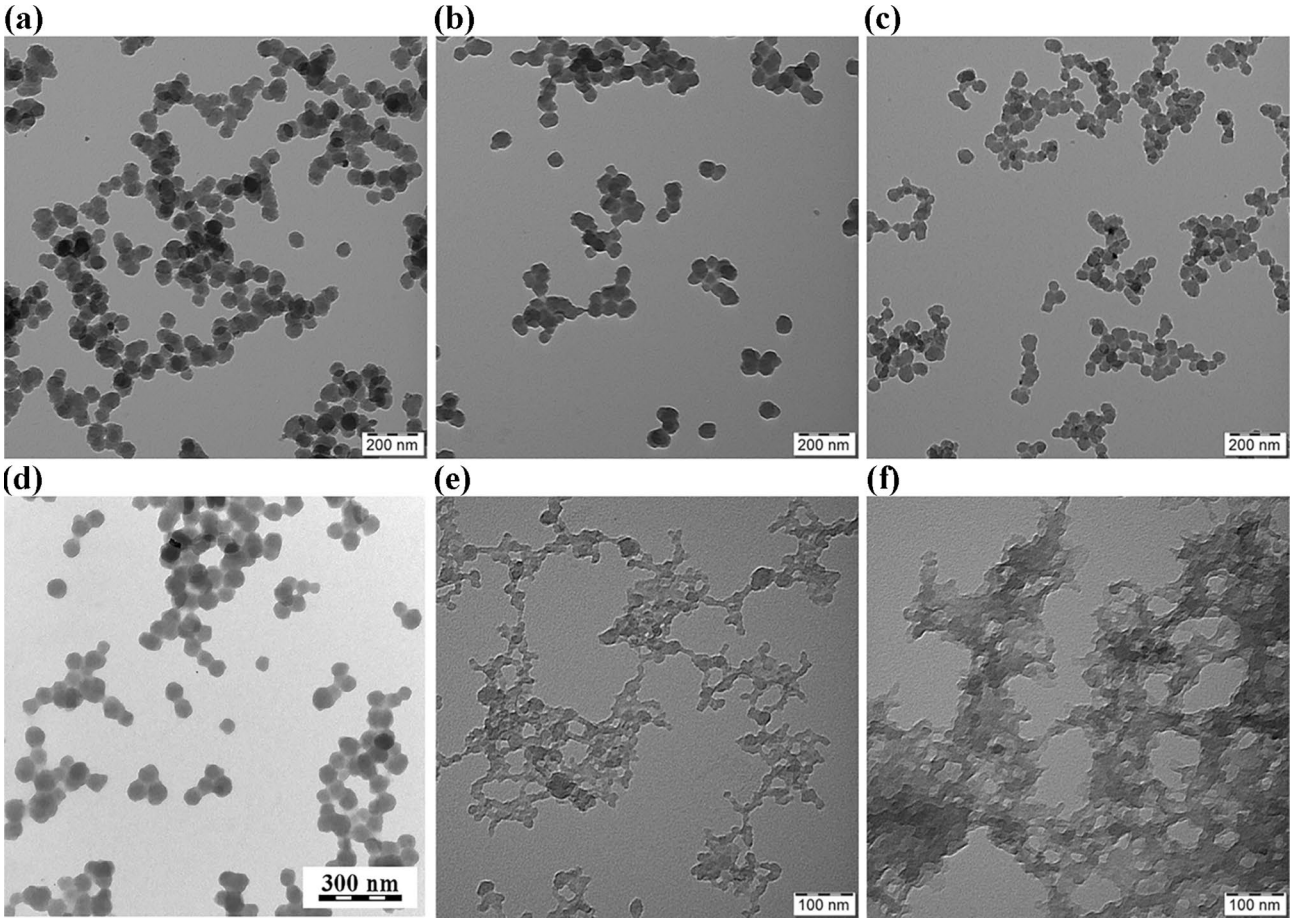

Fig. 3 Comparison of the TEM micrographs of the PPy-NPs prepared in the presence of the polysorbate-based non-ionic emulsifiers, anionic surfactants and PVP at 25 °C. **(a)** 1 wt% Tween 40, **(b)** 1 wt% Tween 60, **(c)** 1 wt% Tween 80, **(d)** 1 wt% PVP, **(e)** 25 mM (corresponding to ~ 1 wt%) SDS, and **(f)** 25 mM (corresponding to ~ 1 wt%) AOT

with DLS measurements. In addition, particle diameter decreased almost regularly with increasing surfactant concentrations, following shape of exponential function $y = a^x$; $0 < a < 1$ (Fig. 4a and Table S3). Nonetheless, a reduction of particle diameter by increasing the concentration of PVP was connected with a noticeable increase of dispersity (Fig. 4a). This can be explained with an increasing viscosity of the polymerization mixture, which caused imbalances in a diffusion of monomers to growing particle nuclei.

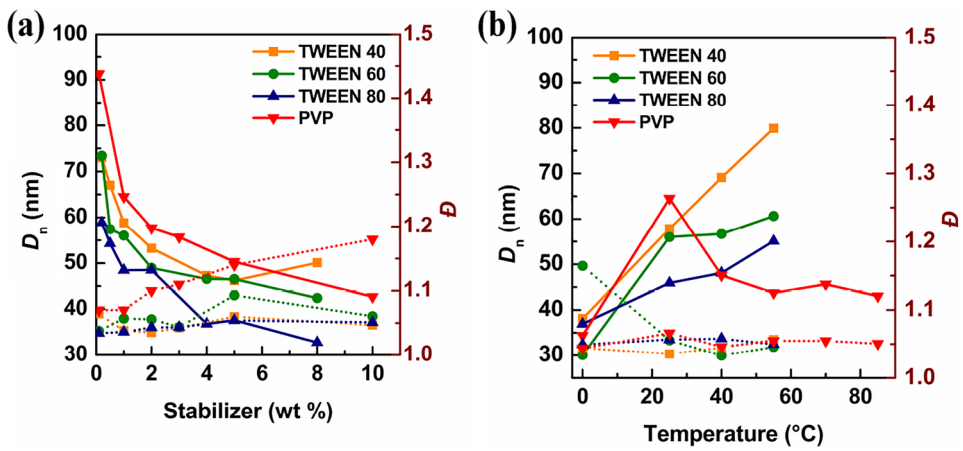

Fig. 4 PPy-NP number-average diameters D_n and dispersity $Đ$ obtained by TEM **(a)** as a function of the stabilizer concentration (25 °C) and **(b)** as a function of reaction temperature. Dotted lines represent the dispersity $Đ$

Next, the effect of the temperature on the size control at one surfactant concentration was investigated (Fig. 4b). A linear increase of the size with increasing temperature from 3 to 60 °C was observed in polymerizations utilizing polysorbate-based surfactants, but not when PVP stabilizer was used. At temperatures above 70 °C polymerization produced a macroscopic precipitate of bulky PPy particles, except when PVP was used. A slight decrease in size with increasing temperature in polymerizations with PVP could be escribed to decrease of viscosity of PVP solution, what led to faster migration of PVP chains to emerging nuclei and consequently to higher number of stabilized growing nuclei. The reverse effect of the temperature on particle diameter in systems with polysorbates can be escribed to an increase of solubility of emulsifier with the temperature, what led to lower number of micelles and consequently to a larger diameter of resulting particles [60]. The morphological properties of the particles are summarized in Fig. S2 and Table S4.

UV–Vis analysis

An application of polysorbate surfactants to control the particles size enforced a replacement of commonly used oxidant $FeCl_3$ (see 3.1.). Therefore, a set of experiments was carried out to examine the effect of the various types and concentrations of oxidizing agents on the particle UV–Vis properties. Two different molar ratios of APS, $FeCl_3$ or H_2O_2 ($n_{Py}/n_{oxidant} = 1/1$ or 1/2.3, respectively) to pyrrole monomers were used in polymerizations. PVP solution (1 wt%) was used as stabilization system, since PVP can act as good dispersion stabilizer for all three oxidants. UV–Vis spectroscopic characteristics of the particles were carried out for wavelengths ranging from 190 to 1100 nm in a physiological PBS buffer at 25 °C (Fig. 5). The characteristic absorption bands with maxima at approximately 440 nm are attributed to the transitions from the valence band to the antibonding polaron state (assigned as a $\pi-\pi^*$ transition). The tail extending to the infrared region with a maximum at approximately 900 nm is attributed to the transition from the valence band to the bipolaron band in all cases. These results corresponded to the published data [62, 63].

The most significant differences in the absorption properties were observed at 600–1100 nm. Shapes of absorption spectra of particles prepared by $FeCl_3$ with different $n_{Py}/n_{Fe(III)}$ molar ratios were almost the same with significant absorptions described above and differed only in the absorption intensity proportionally to $n_{Py}/n_{Fe(III)}$ ratio. On the contrary, when APS at different ratios was used, spectra differed in shapes and absorption intensity decreased with increasing n_{Py}/n_{APS} molar ratio (Fig.**5**). It can be explained by different oxidation mechanisms of the oxidants. $FeCl_3$ causes the one-electron mediated interconnection of the pyrrole units, what results in expansion of $\pi-\pi$ conjugations

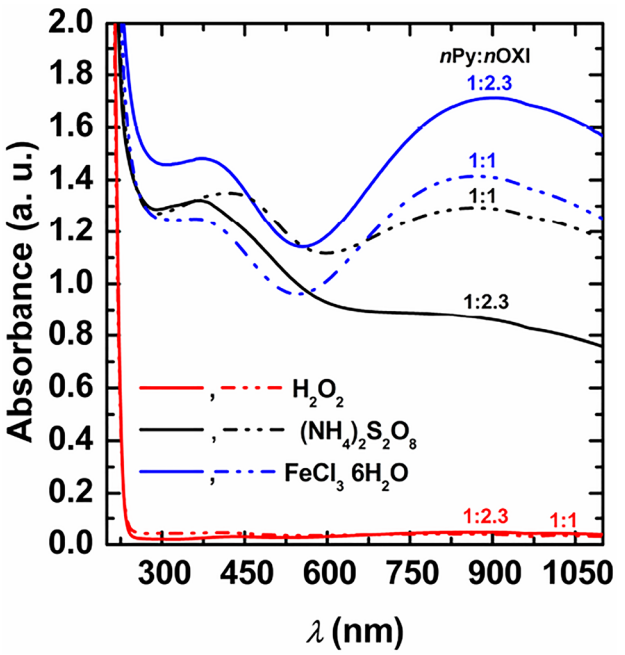

Fig. 5 UV–Vis spectra of the PPy-NPs prepared in 1 wt% PVP with different molar ratios of pyrrole to the oxidant using various oxidants (PBS, pH = 7.4, 25 °C, $c = 110$ µg/mL; $n_{Py}/n_{oxidant} = 1/1$ and 1/2.3)

over the whole polymer chain. Besides that, APS can cause also a direct oxidation of aromatic Py rings and this effect advances with the n_{Py}/n_{APS} ratio. This hypothesis was confirmed by the FTIR/Raman analysis (see next chapter). The strongest effect of the oxidation of aromatic structures was observed when H_2O_2 was used as the oxidant. Absorption intensities of those spectra were found to be about two orders of magnitude weaker. It was thus concluded, that APS can replace $FeCl_3$ opportunely, when its n_{Py}/n_{APS} ratio does not exceed 1/1.

FTIR/Raman analysis

To study the composition and molecular structure of the particles, FTIR and Raman spectroscopy was carried out. Vibrational spectroscopy was used to characterize the product of the pyrrole oxidation by APS and the formation and composition of the nanoparticles prepared in the presence of surfactants [33, 64] (Fig. 6a).

The reaction conditions of the pyrrole oxidation led to the partially deprotonation of the PPy base, as indicated by the three bands of the PPy spectrum at approximately 1552, 1475, and 1189 cm^{-1}, which correspond to the C–C vibrations of the pyrrole rings, the C-N vibrations, and the breathing vibrations of the polypyrrole rings, respectively. These bands are shifted to significantly lower wave numbers in the spectrum of the fully protonated PPy salt. The band at approximately 1692 cm^{-1} indicated the presence of the

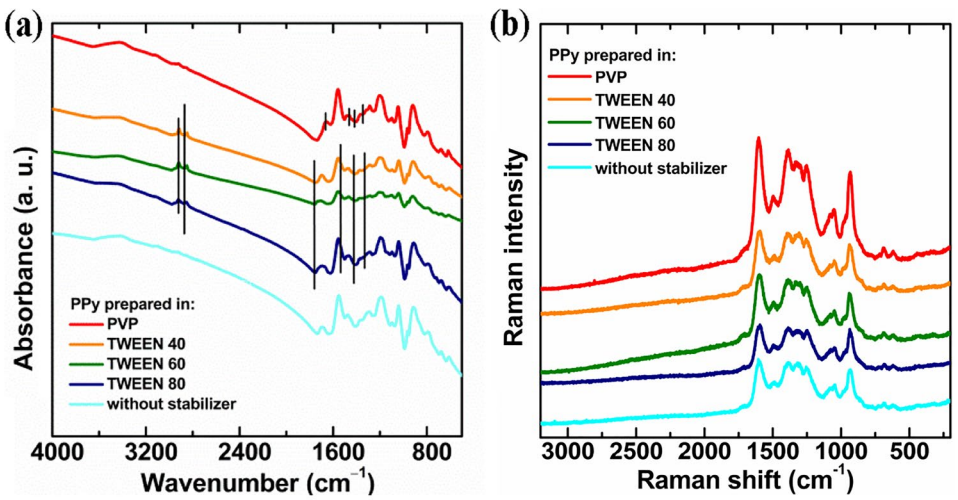

Fig. 6 (**a**) FTIR and (**b**) Raman spectra obtained using 785 nm excitation of the PPy-NPs prepared in 1 wt% solutions of various dispersion stabilizers. Black vertical lines in (a) represent the vibrational bands of the dispersion stabilizers. Light blue lines represent the pure PPy-NPs prepared without stabilizers

carbonyl group at the β-position on the pyrrole ring, which occurred due to the use of a strong oxidation agent.

The FTIR spectra of the PPy-NPs indicated the presence of surfactants. The most intense vibrational band of the spectrum of PVP at 1678 cm^{-1} was attributed to the vibrations of the carbonyl group on the pyrrolidone ring and was also present in the spectrum of the particles stabilized by PVP. Weak but sharp bands at 1462, 1422 and 1287 cm^{-1} were also present. As the bands corresponding to polypyrrole slightly shifted to higher wavenumbers in the spectrum of the sample prepared with PVP, it can be assumed that the presence of PVP further reduced the amount of PPy protonation (Fig. 6a).

Because the molecular structure of all three TWEEN surfactants is similar, their FTIR spectra seemed to be virtually identical. The presence of TWEEN stabilizers in the samples was indicated by the bands at 2923 and 2856 cm^{-1} in the spectra. These bands were attributed to the stretching modes of the aliphatic sequences in the TWEEN structures. The other intense bands characteristic of all the TWEEN spectra at 1146 cm^{-1}, which is assigned to the C–O–C group, overlapped with the spectral features of polypyrrole. Nevertheless, several other weak bands attributed to the TWEEN surfactant were found at 1467 and 1374 cm^{-1}. The positions of the PPy bands remained closer to the band positions corresponding to pure PPy than the bands corresponding to the sample prepared with PVP.

Raman spectroscopy is a method based on inelastic light scattering and provides results that are complementary to the data obtained by the transmission absorption FTIR measurements. The Raman spectra of all the samples were obtained using 785 nm excitation and were similar to each other (Fig. 6b). Despite the unique signal characteristic of PVP and the TWEEN stabilizers, their spectral features were not observed in the spectra of the PPy-NPs, which were obtained using 785 nm excitation. As Raman spectroscopy is a surface sensitive characterization technique, it can be concluded that the concentration of the surfactant on the surface layers of the nanoparticles was lower than that in their matrices. These results show that while the surfactant was removed from the particle surface during washing procedure, a minor portion of the surfactant remained locked inside the particles. The most probably it can be explained by the mechanism of homogeneous nucleation, where the growing polymer nuclei agglomerate simultaneously with their growth and such growing particles enclose some portion of surfactant inside their matrices due to mutual nuclei intergrowth [65]. Missing signals of surfactant molecules in Raman spectra imply that these matrix-locked molecules of surfactant should not affect the physical–chemical properties of particle surfaces.

The band corresponding to the stretching vibrations of C = C bonds and the inter-ring C–C band at approximately 1698 cm^{-1} were located near the position corresponding to the band attributed to deprotonated PPy in the spectra of all the samples. The deprotonation of the prepared PPy-NPs was further confirmed by evaluating the intensity of the band at approximately 1320 cm^{-1}, which was assigned to the neutral units of PPy. This result thus showed, that significant light absorption properties of PPy-NPs at 750–1100 nm do not rely on protonated PPy form. Therefore, the constant intensity of the light absorption in water-based systems with pH varying near to physiological values can be expected.

Conclusion

PPy-NPs were synthesised via water-based redox precipitation/emulsion polymerization technique of pyrrole monomer and ammonium persulphate as an oxidant in the presence of various types of anionic and non-ionic surfactants. This method allows good control of size and

morphology of dispersed PPy-NPs, which is necessary for the biological application. In general, the number-average diameter of the PPy-NPs was controlled from 30 to 100 nm. A step size of 10 nm was achieved by changing the concentration of the non-ionic stabilizers (with an HLB value between 10−16) or polymerization temperature; particle size increased linearly from 30 to 80 nm with rising temperature. Anionic surfactants SDS and AOT allowed a preparation of very stable colloids of PPy-NPs, but their strong solubilizing activity led to formation of particles with soft surfaces prone to sintering in dry state. Experiments showed that a use of ammonium persulphate as an oxidant up to the molar ratio $n_{Py}/n_{oxidant} = 1/1$ was applicable for the preparation of PPy-NPs absorbing light in NIR region with absorption maxima around 900 nm. Since absorption maxima of majority of natural chromophores are below 700 nm, the PPy-NPs can be good candidates as contrast agents for photoacoustic imaging. Absence of vibration bands of surfactants in the Raman spectra confirms a fact that it is possible to wash out the surfactant used for particle preparation from their surface and the synthesis of the particles can be thus followed by additional post synthetic stabilization/surface treatment depending on the requirements of the particle applications.

Funding This work was supported by the Czech Science Foundation (Grant no. 18-05200S).

Compliance with ethical standard

Conflict of interest The authors declare that they have no conflict of interest.

References

1. Wang LX, Li XG, Yang YL (2001) React Funct Polym 47:125–139
2. Le TH, Kim Y, Yoon H (2017) Polymers (Basel) 9(4):150
3. Carquigny S, Segut O, Lakard B, Lallemand F, Fievet P (2008) Synth Met 158:453–461
4. Ren XZ, Zhao Q, Lui JH, Liang X, Zhang QL, Zhang PX, Luo ZK, Gu Y (2008) J Nanosci Nanotechnol 8(5):2643–2646
5. Bengoechea M, Boyano I, Miguel O, Cantero I, Ochoteco E, Pomposo J, Grande H (2006) J Power Sources 160:585–591
6. Camurlu P (2014) RSC Adv 4:55832–55845
7. Hermelin E, Petijean J, Lacroix JC, Chane-Ching KI, Tanguy J, Lacaze PC (2008) Chem Mater 20:4447–4456
8. Son WI, Hong JM, Kim BS (2005) Korean J Chem Eng 22(2):285–290
9. Ekramul Mahmud HNM, Obidul Huq AK, Yahya RB (2016) RSC Adv 6:14778–14791
10. Kausaite-Minkstimiene A, Mazeiko V, Ramanaviciene A, Ramanavicius A (2010) Biosens Bioelectron 26:790–797
11. Ramanaviciene A, Ramanavicius A (2004) Anal Bioanal Chem 379:287–293
12. Humpolíček P, Kašpárková V, Pacherník J, Stejskal J, Bober P, Capáková Z, Radaszkiewicz KA, Junkar I, Lehocký M (2018) Mater Sci Eng C 91:303–310
13. Lee JW, Serna F, Schmidt CE (2006) Langmuir 22:9816–9819
14. Liu H, Li W, Cao Y, Guo Y, Kang Y (2018) J Nanopart Res 20:57
15. Zha Z, Yue X, Ren Q, Dai Z (2013) Adv Mater 25:777–782
16. Wang S, Lin J, Wang T, Chen X, Huang P (2016) Theranostics 6:2394–2413
17. Weber J, Beard PC, Bohndiek SE (2016) Nat Methods 13:639–650
18. Azioune A, Slimane AB, Hamou LA, Pleuvy A, Chehimi MM, Perruchot Ch, Armes SP (2004) Langmuir 20:3350–3356
19. Lin M, Guo CG, Li J, Zhou D, Liu K, Zhang X, Xu TS, Zhang H, Wang LP, Yang B (2014) ACS Appl Mater Interfaces 6:5860–5868
20. Diaz AF, Kanazawa KK, Gardini GP (1979) J Chem Soc Chem Commun 14:635–636
21. Li Y, Dong S (1993) J Electroanal Chem 348:181–188
22. Gao Z, Bobacka J, Lewenstam A, Ivaska A (1994) Electrochim Acta 39:755–762
23. Myers RE (1986) J Electron Mater 15:61–69
24. Armes SP (1987) Synth Met 20:365–371
25. Chaudhary V, Sharma S (2019) J Polym Res 26:102
26. Yang X, Lu Y (2005) Mater Lett 59:2484–2487
27. Ramanavicius A, Karabanovas V, Ramanaviciene A, Rotomskis R (2009) J Nanosci Nanotechnol 9:1909–1915
28. Jang J, Lee K (2002) Chem Commun 2:1098–1099
29. Thiéblemont JC, Brun A, Marty J, Planche MF, Calo P (1995) Polymer (Guildf) 36:1605–1610
30. Nishio K, Fujimoto M, Ando O, Ono H, Murayama T (1996) J Appl Electrochem 26:425–429
31. Kudoh Y (1996) Synth Met 79:17–22
32. Omastová M, Trchová M, Kovářová J, Stejskal J (2003) Synth Met 138:447–455
33. Blinova NV, Stejskal J, Trchová M, Prokeš J, Omastová M (2007) Eur Polym J 43:2331–2341
34. Ovando-Medina VM, Peralta RD, Mendizábal E, Martínez-Gutiérrez H, Lara-Ceniceros TE, Ledezma-Rodríguez R (2011) Colloid Polym Sci 289:759–765
35. Hazarika J, Kumar A (2013) Synth Met 175:155–162
36. Leonavicius K, Ramanaviciene A, Ramanavicius A (2011) Langmuir 27:10970–10976
37. Meng S, Zhang Z, Rouabhia M (2010) Synth Met 160:116–122
38. Selvaraj M, Palraj S, Maruthan K, Rajagopal G, Venkatachari G (2009) J Appl Polym Sci 116:1524–1537
39. Shinde SS, Gund GS, Dubal DP, Jambure SB, Lokhande CD (2014) Electrochim Acta 119:1–10
40. Pron A, Wojnar K (1987) Electron Prop Conjug Polym 76:291–293
41. Sari B, Gök A, Şahin D (2006) J Appl Polym Sci 101:241–249
42. Omastová M, Bober P, Morávková Z, Peřinka N, Kaplanová M, Syrový M, Hromádková J, Trchová M, Stejskal J (2014) Electrochim Acta 122:296–302
43. DeArmitt C, Armes SP (1993) Langmuir 9(3):652–654
44. Samanta D, Meiser JL, Zare RN (2015) Nanoscale 7:9497–9504
45. Wen J, Tian Y, Mei Z, Wu W, Tian Y (2017) RSC Adv 7:53219–53225
46. Woo HY, Jung WG, Ihm DW, Kim JY (2010) Synth Met 160:588–591
47. Kim S, Oh WK, Jeong YS, Hong JY, Cho BR, Hanh JS, Jang J (2011) Biomaterials 32:2342–2350
48. Hong JY, Yoon H, Jang J (2010) Small 6:679–686
49. Wang Q, Wang J, Lv G, Wang F, Zhou X, Hu J, Wang Q (2014) J Mater Sci 49:3484–3490

50. Abbasi AMR, Marsalkova M, Militky J (2013) J Nanoparticles 2013:1–4
51. Ødegård R, Skotheim TA, Lee HS (1991) J Electrochem Soc 138:2930–2934
52. Xing S, Zhao G (2007) e-Polymers 7(1)
53. Hoshina Y, Zaragoza-Contreras EA, Farnood R, Kobayashi T (2012) Polym Bull 68:1689–1705
54. Kwon WJ, Suh DH, Chin BD, Yu JW (2008) J Appl Polym Sci 110:1324–1329
55. Griffin WC (1955) Am Perfumer Essential Oil Rev 65(5):26–29
56. Rowe EL (1965) J Pharm Sci 54:260–264
57. Holmberg K (2003) Surfactants and polymers in aqueous solution, 2nd edn. Wiley Ltd, Chichester, UK
58. Linder M, Bäumler M, Stäbler A (2018) Coatings 8(12):469–487
59. Housaindokht MR, Pour AN (2012) Solid State Sci 14:622–625
60. Farn RJ (2006) Chemistry and technology of surfactants. Blackwell Publishing Ltd, Oxford, UK
61. Gilbert RG, Hess M, Jenkins AD, Jones RG, Kratochvíl P, Stepto RFT (2009) Pure Appl Chem 81:351–353
62. Brédas JL, Scott JC, Yakushi K, Street GB (1984) Phys Rev B 30:1023–1025
63. Foroughi J, Spinks GM, Wallace GG (2009) Synth Met 158:1837–1843
64. Trchová M, Stejskal J (2018) J Phys Chem A 122:9298–9306
65. Fitch RM (1973) Br Polym J 5:467–483